MAI Analysis of an Asynchronous MC-CDMA System With Polarization Diversity

Xuan Li
School of Engineering Systems
Queensland University of Technology
Brisbane, Australia 4000
Email: x4.li@qut.edu.au

Yu Chieh Huang
School of Engineering Systems
Queensland University of Technology
Brisbane, Australia 4000
Email: by.huang@qut.edu.au

Bouchra Senadji
School of Engineering Systems
Queensland University of Technology
Brisbane, Australia 4000
Email: b.senadji@qut.edu.au

***Abstract*—The use of polarization antenna diversity techniques in mobile communications can improve system robustness against multipath fading. However, when used in asynchronous CDMA transmission, an increase in the carrier to noise ratio (CNR) does not automatically imply an increase in the received signal to noise ratio (SNR), due to the possibility of an increase in multiple access interference (MAI). We present a derivation of the signal to interference plus noise ratio (SINR) and calculate the average bit error rate (BER) of an uplink MC-CDMA system using polarization diversity reception at the base station. The results show that even though the use of polarization diversity introduces additional MAI, the resulting increase in the signal power was able to give an overall improvement in the performance of the SNR and average BER.**

I. Introduction

A microwave radio signal in a mobile communications channel typically exhibits extreme amplitude variations as a result of multipath propagation [1]. Fades which are 40dB below the mean signal level are common and makes this type of communications difficult [2]. The use of antenna diversity schemes directly mitigates the effects of the mobile channel without the consumption of additional spectra, at the expense of additional RF equipment [3].

Antenna diversity introduces signal redundancy across multiple antennas to improve system robustness against multipath fading by increasing the carrier to noise ratio (CNR) [4]. For asynchronous CDMA systems, an improvement in the CNR post recombination does not automatically imply an increase in system performance. Antenna diversity does not compensate for asynchronous transmission, which causes user codes to lose orthogonality and introduce multiple access interference (MAI).

In this paper, we analyze the additional MAI introduced as a result of using antenna polarization diversity in a multi carrier (MC) CDMA system. The resulting expressions for the signal to interference plus noise ratio (SINR) and average bit error rate (BER) are derived.

Signaling and antenna based diversity techniques have been well documented in the literature [1]. In typical systems using spatial diversity, an antenna separation in the order of 30 wavelengths is required to achieve sufficient decorrelation for diversity action at the base station [5]. Due to space availability, this type of diversity may be difficult to implement. The use of antenna polarization diversity is seen as a better alternative because it allows antenna elements to be co-located [5], [6].

In polarization diversity, signal redundancy is achieved by the reception of orthogonally polarized electromagnetic waves that have uncorrelated signal envelopes [5], [6], [7]. Results in the published literature have shown that the envelope correlation of polarization diversity branches are close to zero, and the performance is comparable to that of space diversity [4].

Polarization diversity has traditionally utilized linear vertically (Vpol) and horizontally (Hpol) polarized antennas. One limitation of this configuration is the intrinsic power imbalance between diversity branches [8]. Asymmetric attenuation in the Vpol and Hpol may lead to significant power imbalance and degrade diversity performance [5], [7]. To overcome this, linear polarized antenna elements which are aligned at an angle $\pm\alpha$ relative to the vertical, have been proposed to equalize the power imbalance [6]. This diversity antenna configuration is used in our discussion.

MC-CDMA has been proposed as one of the candidate multiple access schemes in 4G systems. The main idea of MC-CDMA is to transmit a single data stream over a number of lower rate subcarriers that have been uniquely coded by a spreading sequence across the frequency domain [9]. Advantages of MC-CDMA include the ability to counter the frequency selective nature of the channel, which was a problem for Direct Sequence (DS) CDMA. Extended symbol durations allow for quasi synchronization, giving more robustness against inter symbol interference (ISI) and inter chip interference (ICI) [10]. Further, if orthogonal subcarriers with overlapping sidebands are used, spectral efficiency is facilitated [11]. However, because spreading is done in the frequency domain, MC-CDMA does not inherently introduce frequency diversity [12], calling the need to use other forms of diversity. One of the motivations of this paper is to introduce antenna polarization diversity in MC-CDMA.

Our development considers an uplink MC-CDMA system using a $\pm\alpha$ receiver antenna configuration. MAI analysis is central to this investigation since synchronous transmission is not guaranteed in the uplink. The effect of the additional MAI from diversity is incorporated into the study and we show that

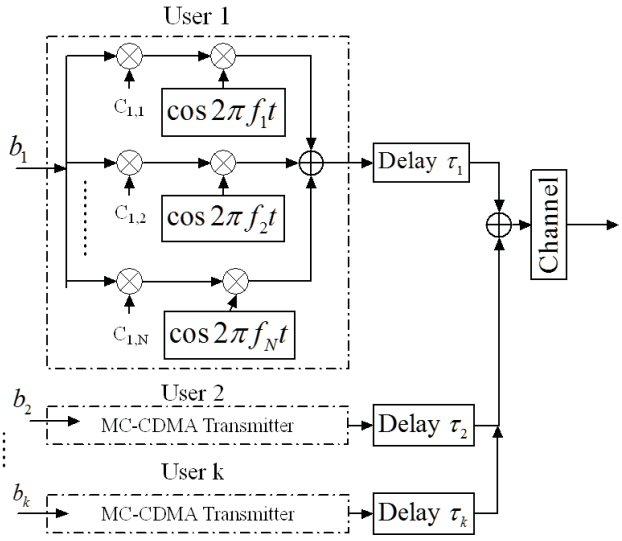

Fig. 1. Block Diagram of the MC-CDMA transmitter

despite an increase in MAI, the increase in signal power due to polarization diversity was able to give an overall improvement in system performance.

II. System Model

This section presents a mathematical model of the uplink MC-CDMA using polarization diversity at the receiver.

A. Transmitter

Fig. 1 illustrates the block diagram of a MC-CDMA transmitter. The data bits of the kth user, b_k, is assumed to be a BPSK modulated waveform and is first replicated in parallel over N subcarriers. The number of subcarriers is dictated by the spreading gain of the pseudo-random (PN) spreading sequence $c_{k,i}$. The PN code is applied in the frequency domain across the N orthogonal subcarriers, with the ith chip being assigned to the ith subcarrier. In other words, given a spreading sequence of length N $\{c[1], c[2], \ldots, c[N]\}$, subcarrier branch $f_{k,1}$ is assigned $c[1]$, while subcarrier branch $f_{k,2}$ assigned with $c[2]$ and so forth for the N subcarriers. It is important to note that in MC-CDMA, the resulting symbol duration T_s is equal to the chip duration, and thus, given the appropriate choice in the number of carriers occupying the available bandwidth, it is reasonable to assume that each subcarrier signal is experiencing frequency flat fading [9]. It is also assumed that channel conditions remain unchanged over two consecutive symbols. After spreading is done across the frequency domain, each carrier is modulated to its assigned subcarrier frequency, $f_{k,i}$, combined, and transmitted through the transmission medium.

The transmitted signal of user k, s_k, is written as follows:

$$s_k(t) = \sum_{i=1}^{N} \sqrt{2P} b_k c_{k,i} \cos\left(2\pi f_{k,i} t + \phi_{k,i}(t)\right), \quad (1)$$

where P is the power transmitted in each subcarrier and $\phi_{k,i}(t)$ is the random phase introduced by the modulator. In this case, the power is assumed to be the same across all N subcarriers.

B. Receiver

At the base station receiver, the modeling of polarization diversity reception is based on the $\pm\alpha$ configuration outlined in [6]. The transmitted signal is assumed to be principally vertically polarized. Due to multipath signal propagation within the transmission medium, rotation of the polarization states are induced [6], [8], and causes the signal received at the base station to have both vertical and horizontally polarized components, $r_{k,v}(t)$ and $r_{k,h}(t)$ respectively.

$$r_{k,v}(t) = \sum_{i=1}^{N} \sqrt{2P}\beta_{k,v,i} b_k c_{k,i} \cdot \cos\left[2\pi f_i (t-\tau_k) + \phi_{k,i}(t) + \theta_{k,v,i}\right] \quad (2)$$

$$r_{k,h}(t) = \sum_{i=1}^{N} \sqrt{2P}\beta_{k,h,i} b_k c_{k,i} \cdot \cos\left[2\pi f_i (t-\tau_k) + \phi_{k,i}(t) + \theta_{k,h,i}\right] \quad (3)$$

$\theta_{k,v,i}$ and $\theta_{k,h,i}$ represent the random phase induced by the channel in the vertical and horizontal polarizations, and are assumed to be uniformly distributed between $[0, 2\pi)$. $\beta_{k,v,i}$ and $\beta_{k,h,i}$ are the channel attenuation coefficients in the Vpol and Hpol, respectively. They are modeled as Rayleigh random variables, and are assumed to be independent between polarizations [6], [7], and independent between users [13]. The relationship between $\beta_{k,v,i}$ and $\beta_{k,h,i}$ is defined by the cross polarization discrimination (XPD), Γ , which is the ratio between the received power in the Vpol and the received power in the Hpol [6],

$$\Gamma = \frac{E\left[\beta_{r,v,i}^2\right]}{E\left[\beta_{r,h,i}^2\right]}, \quad (4)$$

where $E[\cdot]$ is the expectation operator. These assumptions are verified with the experimental results presented in [5] and [6].

Due to the asynchronous nature in uplink transmission, a time delay τ_k is introduced and is assumed to be uniformly distributed between $[0, T_s)$. The time delay for the reference user, τ_r is defined to be zero.

A polarization diversity antenna composed of two elements V_1 and V_2 which form an angle of $\pm\alpha$ relative to the vertical axis is used. Azimuthal dependence of the kth mobile user is introduced by the ϑ_k parameter. The geometry of the system is illustrated in Fig. 2. Upon reception, signals of the vertical and horizontal polarizations are projected onto the V_1 and V_2 antenna components [6].

$$V_1 = r_{k,h}(t)\sin\alpha\cos\vartheta_k + r_{k,v}(t)\cos\alpha \quad (5)$$

$$V_2 = -r_{k,h}(t)\sin\alpha\cos\vartheta_k + r_{k,v}(t)\cos\alpha \quad (6)$$

The receiver structure takes advantage of the two diversity branches provided through the $\pm\alpha$ antenna elements, and uses post detection combining. The general MC-CDMA receiver block diagram is illustrated in Fig. 3. The received signal

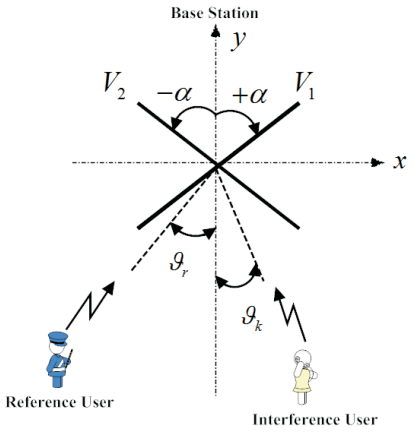

Fig. 2. Goemetry of the $\pm\alpha$ antenna configuration

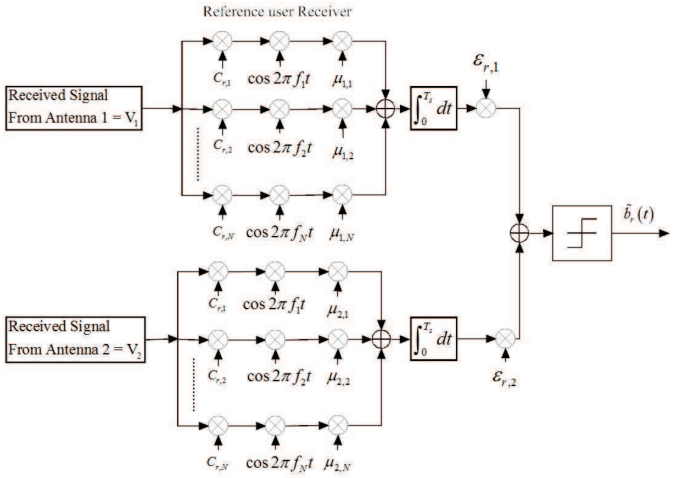

Fig. 3. Block diagram of the MC-CDMA receiver with polarization diversity

in each of the subcarriers of both antennas are despread, demodulated, weighted and combined, before being passed into the correlation receivers. The two correlator test statistics are then weighted, combined and input through a decision device to determine the transmitted bit.

The output test statistics of the correlation receivers Z_1 and Z_2 for antenna branches V_1 and V_2 respectively are calculated as:

$$\begin{aligned} Z_1 &= \int_0^{T_s} V_1 \sum_{i=1}^{N} c_{r,i} \cos\left(2\pi f_{r,i} t\right) \mu_{1,i}\, dt \\ &= D_1 + \mathrm{MAI}_1 + \eta_1 \end{aligned} \tag{7}$$

$$\begin{aligned} Z_2 &= \int_0^{T_s} V_2 \sum_{i=1}^{N} c_{r,i} \cos\left(2\pi f_{r,i} t\right) \mu_{2,i}\, dt \\ &= D_2 + \mathrm{MAI}_2 + \eta_2 \,. \end{aligned} \tag{8}$$

$\mu_{1,i}$ and $\mu_{2,i}$ are the combining gain parameters used to weight each of the individual subcarriers in antenna V_1 and V_2 respectively. Equal gain combining (EGC) is used across the subcarriers such that $\mu_{1,i} = \mu_{2,i} = \mu_i$ for $i = 1 \ldots N$.

The test statistics Z_1 and Z_2 can be written as the sum of the desired signal, D; the MAI component; and the additive white Gaussian noise (AWGN), η. The desired signal in V_1 and V_2 are calculated as follows:

$$D_1 = \sqrt{\frac{P}{2}} b_{r,0} \sum_{i=1}^{N} \mu_i \left[\beta_{r,h,i} A_r + \beta_{r,v,i} \Psi\right] \tag{9}$$

$$D_2 = \sqrt{\frac{P}{2}} b_{r,0} \sum_{i=1}^{N} \mu_i \left[-\beta_{r,h,i} A_r + \beta_{r,v,i} \Psi\right] . \tag{10}$$

We define $A_k = \sin\alpha \cos\vartheta_k$ and $\Psi = \cos\alpha$. Because we are dealing with the reference user, $k = r$, $A_r = \sin\alpha\cos\vartheta_r$. We also define $b_{r,0}$ as the current data bit of the reference user.

The noise interference terms, η_1 and η_2 are the result of the AWGN channel with a noise power spectral density of N_0. In general, the statistics of η_1 and η_2 will not be the same, and depends on the combining gains $\mu_{1,i}$ and $\mu_{2,i}$. Since EGC is used across the subcarriers, the statistics of η_1 and η_2 are assumed to be the same and have zero mean with a variance of:

$$\mathrm{var}\left(\eta_1\right) = \mathrm{var}\left(\eta_2\right) = \frac{N_0 T_s}{4} \sum_{i=1}^{N} \mu_i^2 \,. \tag{11}$$

The MAI term is the undesired term as a result of multiple access interference. The MAI term can be separated and analyzed in two parts, I and J [13]. I represents the contribution of MAI from the other $K-1$ users using the same subcarrier frequencies, while J is the contribution of MAI from other users with different subcarrier frequencies. I and J for antennas V_1 and V_2 are calculated as:

$$\begin{aligned} I_1 =& \sqrt{\frac{P}{2}}\, T_s \sum_{\substack{k=1 \\ k\neq r}}^{K} \left[b_{k,-1}\tau_k + b_{k,0}\left(T_s - \tau_k\right)\right] \\ & \cdot \sum_{i=1}^{N} c_{k,i} c_{r,i} \mu_i \left[\beta_{k,v,i} \cos\zeta_{k,v,i} \Psi + \beta_{k,h,i} \cos\zeta_{k,h,i} A_k\right] \end{aligned} \tag{12}$$

$$\begin{aligned} I_2 =& \sqrt{\frac{P}{2}}\, T_s \sum_{\substack{k=1 \\ k\neq r}}^{K} \left[b_{k,-1}\tau_k + b_{k,0}\left(T_s - \tau_k\right)\right] \\ & \cdot \sum_{i=1}^{N} c_{k,i} c_{r,i} \mu_i \left[\beta_{k,v,i} \cos\zeta_{k,v,i} \Psi - \beta_{k,h,i} \cos\zeta_{k,h,i} A_k\right] , \end{aligned} \tag{13}$$

and,

$$\begin{aligned} J_1 =& \sqrt{2P} \sum_{\substack{k=1 \\ k\neq r}}^{K} \left(b_{k,-1} - b_{k,0}\right) \sum_{i=1}^{N} \mu_i \sum_{\substack{j=1 \\ j\neq i}}^{N} \frac{c_{k,j} c_{r,i}}{2\Delta_{i,j}} \\ & \cdot \left\{ \begin{array}{l} \beta_{k,v,j} \Psi \left[\sin\left(\Delta_{i,j}\tau_k + \zeta_{k,v,j}\right) - \sin\zeta_{k,v,j}\right] \\ +\beta_{k,h,j} A_k \left[\sin\left(\Delta_{i,j}\tau_k + \zeta_{k,h,j}\right) - \sin\zeta_{k,h,j}\right] \end{array} \right\} \end{aligned} \tag{14}$$

$$J_2 = \sqrt{2P}\sum_{\substack{k=1\\k\neq r}}^{K}\left(b_{k,-1}-b_{k,0}\right)\sum_{i=1}^{N}\mu_i\sum_{\substack{j=1\\j\neq i}}^{N}\frac{c_{k,j}c_{r,i}}{2\Delta_{i,j}} \cdot\left\{\begin{array}{l}\beta_{k,v,j}\Psi\left[\sin\left(\Delta_{i,j}\tau_k+\zeta_{k,v,j}\right)-\sin\zeta_{k,v,j}\right]\\ -\beta_{k,h,j}A_k\left[\sin\left(\Delta_{i,j}\tau_k+\zeta_{k,h,j}\right)-\sin\zeta_{k,h,j}\right]\end{array}\right\}. \quad (15)$$

$b_{k,-1}$ and $b_{k,0}$ are used to represent the previous and current data bits of user k respectively. The ζ parameters have been introduced to account for the total combined phase, where $\zeta_{k,v,i} = \phi_{k,i}(t) + \theta_{k,v,i}(t) - 2\pi f_{k,i}\tau_k$. Further, the spectral distance between the ith and jth subcarrier is defined to be:

$$\Delta_{i,j} = \frac{2\pi\left(i-j\right)}{T_s}. \quad (16)$$

Maximal ratio combining (MRC) is employed to combine the signals across the two antennas. The combining gain parameters $\varepsilon_{r,1}$ and $\varepsilon_{r,2}$ are used to weight the two branches according to their signal to noise power ratios and then summed [1].

$$\varepsilon_{r,1} = B_{r,h}A_r + B_{r,v}\Psi \quad (17)$$

$$\varepsilon_{r,2} = -B_{r,h}A_r + B_{r,v}\Psi \quad (18)$$

For ease in representation, $\sum_{i=1}^{N}\beta_{r,h,i}$ and $\sum_{i=1}^{N}\beta_{r,v,i}$ have been replaced by $B_{r,h}$ and $B_{r,v}$ respectively.

In the derivation for the expression of the SINR, we start with the power of the desired signal, post MRC, calculated as:

$$D^2 = \left(D_1\varepsilon_{r,1}+D_2\varepsilon_{r,2}\right)^2 = \frac{P}{2}b_{r,0}^2\left[\begin{array}{l}\left(A_rB_{r,h}\sum_{i=1}^{N}\mu_i\right)\left(\varepsilon_{r,1}-\varepsilon_{r,2}\right)\\ +\left(\Omega_rB_{r,v}\sum_{i=1}^{N}\mu_i\right)\left(\varepsilon_{r,1}+\varepsilon_{r,2}\right)\end{array}\right]^2. \quad (19)$$

The total MAI power ρ_{MAI} is calculated by the summation of the power from I and J. We represent these as ρ_I and ρ_J respectively.

$$\rho_{\mathrm{MAI}} = \rho_I + \rho_J \quad (20)$$

ρ_I and ρ_J are calculated by taking the second order moment of I and J. The central limit theorem allows the treatment of I and J as independent Gaussian random variables with zero mean and variance σ^2 [13].

$$\rho_I = E\left[I^2\right] = \left(K-1\right)\frac{PT_s^2\sigma^2}{3}\cdot\left[\frac{\overline{A}^2}{\Gamma}\left(\varepsilon_{r,1}-\varepsilon_{r,2}\right)^2+\Psi^2\left(\varepsilon_{r,1}+\varepsilon_{r,2}\right)^2\right]\sum_{i=1}^{N}\mu_i^2 \quad (21)$$

$$\rho_J = E\left[J^2\right] = \left(K-1\right)\frac{PT_s^2\sigma^2C}{2\pi^2}\cdot\left[\frac{\overline{A}^2}{\Gamma}\left(\varepsilon_{r,1}-\varepsilon_{r,2}\right)^2+\Psi^2\left(\varepsilon_{r,1}+\varepsilon_{r,2}\right)^2\right]\sum_{i=1}^{N}\mu_i^2, \quad (22)$$

where, $\overline{A}^2 = E\left[\cos^2\vartheta_k\right]\sin^2\alpha$ and

$$C = \frac{1}{N}\sum_{i=1}^{N}\sum_{\substack{j=1\\j\neq i}}^{N}\frac{1}{(i-j)^2}. \quad (23)$$

The calculation of the SINR, γ_{p1}^2, incorporates the additional MAI from polarization diversity as a source of interference. The SINR is derived by taking the ratio between the desired signal and the sum of all interference terms.

$$\gamma_{p1}^2 = \frac{D^2}{\rho_{MAI}+\mathrm{var}(\eta_1)\varepsilon_{r,1}^2+\mathrm{var}(\eta_2)\varepsilon_{r,2}^2} \quad (24)$$

We assume that channel conditions are known exactly at the receiver and evaluate the instantaneous BER conditional to the state of the channel. Because both type of MAI has been approximated to be independent Gaussian random variables with zero mean, we evaluate the instantaneous BER as:

$$p_e^{p1}|B_{r,h},B_{r,v} = Q\left(\gamma_{p1}\right), \quad (25)$$

where $Q(\cdot)$ is one minus the cumulative distribution function of the standardized normal random variable. For the sake of simplicity in the calculations to follow, the EGC parameters μ_i are all set to be unity.

To calculate the average BER, we have to take the expectation over all of the variables involved, namely $B_{r,h}$ and $B_{r,v}$.

$$E\left[p_e^{p1}\right] = \int_{-\infty}^{+\infty}\int_{-\infty}^{+\infty}Q\left(\gamma_{p1}\right)\cdot prob\left(B_{r,h}\,B_{r,v}\right)\,dB_{r,h}\,dB_{r,v} \quad (26)$$

Since it was assumed that the fading in the Vpol and Hpol are independent of each other, the joint distribution can be written as the product of their respective distributions, $prob\left(B_{r,h}\right)$ and $prob\left(B_{r,v}\right)$.

$$E\left[p_e^{p1}\right] = \int_{-\infty}^{+\infty}\int_{-\infty}^{+\infty}Q\left(\gamma_{p1}\right)\cdot prob\left(B_{r,h}\right)\cdot prob\left(B_{r,v}\right)\,dB_{r,h}\,dB_{r,v} \quad (27)$$

Here, $B_{r,h}$ and $B_{r,v}$ represent a sum of N Rayleigh random variables. It is of interest to note at this point that the Rayleigh distribution is a special case of the Nakagami-m distribution, with m being equal to unity. Thus, an interpretation for $B_{r,h}$ and $B_{r,v}$ is that we have a sum of m-variables. When the branches are assumed to have independent fading, the probability density functions of $B_{r,h}$ and $B_{r,v}$ can be approximated with the Nakagami-m distribution [14],

$$prob\left(B_{r,h}\right) = \frac{2}{\Gamma\left(m\right)}\left(\frac{m}{\Omega_h}\right)^m B_{r,h}^{2m-1}\exp\left(-\frac{m}{\Omega_h}B_{r,h}^2\right) \quad (28)$$

$$prob\left(B_{r,v}\right) = \frac{2}{\Gamma\left(m\right)}\left(\frac{m}{\Omega_v}\right)^m B_{r,v}^{2m-1}\exp\left(-\frac{m}{\Omega_v}B_{r,v}^2\right), \quad (29)$$

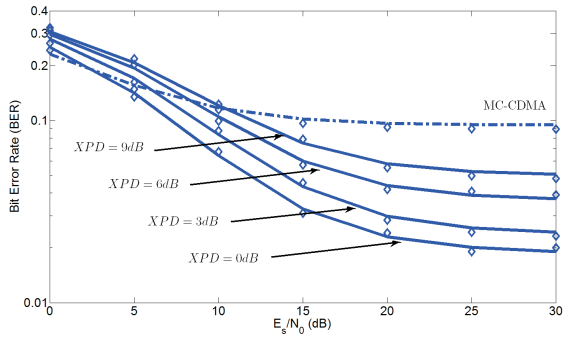

Fig. 4. BER for asynchronous MC-CDMA using polarization diversity with different values of the XPD. ($N = K = 16$, $\alpha = \pi/4$ and $\vartheta_k = 0$)

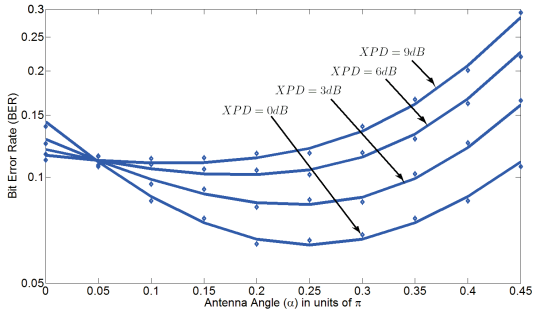

Fig. 5. BER for asynchronous MC-CDMA using polarization diversity with different values of α. ($N = K = 16$, $E_b/N_0 = 10$dB and $\vartheta_k = 0$)

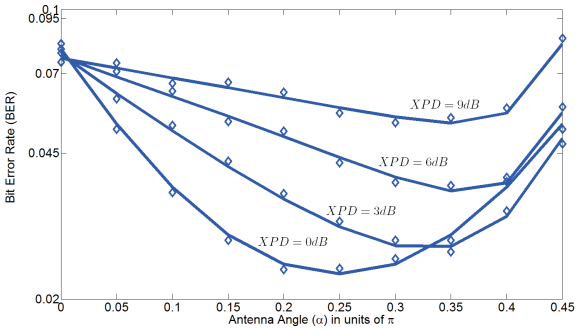

Fig. 6. BER for asynchronous MC-CDMA using polarization diversity with different values of α. ($N = K = 16, E_b/N_0 = 20$dB and $\vartheta_k = 0$)

with the parameters of the m distribution given as:

$$\Omega_v = E\left[B_{r,v}^2\right] \approx \frac{8N^2\sigma^2}{5} \tag{30}$$

$$\Omega_h = E\left[B_{r,h}^2\right] \approx \frac{8N^2\sigma^2}{5\Gamma} \tag{31}$$

$$m = \frac{\Omega_h^2}{\mathrm{Var}\left[B_{r,h}^2\right]} = \frac{\Omega_v^2}{\mathrm{Var}\left[B_{r,v}^2\right]} \approx N\,. \tag{32}$$

The double integral for the average BER can not be evaluated analytically, however, because $prob\,(B_{r,h})$ and $prob\,(B_{r,v})$ have been approximated with the Nakagami-m distribution, numerical methods may be applied. Our calculation follows the same approach as the one that was used in [13], and we employ the Monte Carlo integration technique using the traditional algorithm [15].

III. Results and Discussions

Monte Carlo simulations are used to verify the validity of the development. A full user system, $N = 16$, is assumed and the Rayleigh parameter for the channel is set to 0.5. One million realizations were used in the simulation. These results have been presented with different values of the XPD. For the ease of comparison, the performance of the basic asynchronous MC-CDMA system is also shown.

Fig. 4 verifies that the use of polarization diversity for asynchronous MC-CDMA does not always guarantee an improvement in the average BER performance. For the scenario with XPD of 9dB, $\alpha = \frac{\pi}{4}$ and $\vartheta_k = 0$, polarization diversity does not offer an improvement in the average BER until the value of E_b/N_0 exceeds 10dB. Under optimal conditions with equal reception power across the Vpol and Hpol such that $\Gamma = 0$dB, MC-CDMA using polarization diversity does not start to out perform basic MC-CDMA until the threshold at 5dB.

These results also emphasize that performance increases when power imbalance is equalized. This remains consistent with the results in [6]. In practice the absence of power imbalance rarely exists, particularly in suburban environments where the XPD can exceed values greater than 10dB [8].

Based on the interpretation of [6] on the effects of varying α, we can conclude that manual adjustment of the antenna alignment may be used to further weight the contributions in diversity of the Vpol and Hpol. This angle dependency is studied in the second part of our discussion.

Fig. 5 and Fig. 6 present the effect of the antenna angle α with different values of E_b/N_0 upon average BER performance. Both of the figures indicate that under the influence of XPD, the use of $\alpha = \frac{\pi}{4}$, a value that has been widely applied in the literature [16], [17], [18], does not guarantee the best performance for MC-CDMA with polarization diversity.

This is especially evident in Fig. 6, where we see that the use of $\alpha = \frac{\pi}{4}$ is suboptimal when there is power imbalance between the Vpol and Hpol. Further, the results show that performance may be optimized by increasing the angle α with respect to the y axis. The interpretation for this is that we are projecting more of the Hpol component onto antennas V_1 and V_2, while reducing the Vpol component contributions in an attempt to provide artificial power equalization. This interpretation remains consistent with the antenna weighting contribution concept outlined in [6].

At first glance, the results presented in Fig. 5 appear to contradict the explanations, where optimal values of α have decreased. The explanation for this is that Fig. 5 presents the performance at a $E_b/N_0 = 10$dB value that is close to the performance threshold. In essence, the results indicate that the

interference due to the MAI in the Vpol and Hpol dominates the benefits gained from power equalization, causing performance to degrade.

Even though the results do predict a deterioration in performance for values of E_b/N_0 close to the threshold. It is important to note that for values greater than the 10dB threshold with moderate values of the XPD, the use of antenna polarization diversity is capable of providing significant reductions in the average BER.

Both figures also verifies the fact that while the power between the Vpol and Hpol are balanced, optimal antenna alignment is given at $\alpha = \frac{\pi}{4}$.

IV. Conclusion

An asynchronous MC-CDMA system using base station polarization diversity was discussed. We showed that the introduction of polarization diversity to overcome the effects of fading was outperformed by the basic MC-CDMA system for low values of E_b/N_0. The results verify our hypothesis that the introduction of signal diversity can introduce significant additional MAI that adversely effects system performance. This result emphasizes the need to consider antenna diversity as a source of MAI. In the general scenario though, the gains provided by polarization diversity was able to overcome the additional interference due to MAI, to give overall improvement in average BER.

In our discussions, we also verified that excess power imbalance between Vpol and Hpol can have significant adverse effects on the average BER. Adjustments in the antenna configuration by varying α is shown to be able to further optimally weight the signals received through the vertical and horizontal polarizations.

References

[1] W. C. Jakes, *Microwave mobile communications*. Piscataway, N.J : IEEE Press, [1994], c1974., 1974.

[2] V. Fung, T. S. Rappaport, and B. Thoma, "Bit error simulation for $\pi/4$ dqpsk mobile radio communications using two-ray and measurement-based impulse response models," *Selected Areas in Communications, IEEE Journal on*, vol. 11, no. 3, pp. 393–405, 1993.

[3] R. G. Vaughan and J. B. Andersen, "Antenna diversity in mobile communications," *Vehicular Technology, IEEE Transactions on*, vol. 36, no. 4, pp. 149–172, 1987.

[4] J. Dietrich, C. B., K. Dietze, J. R. Nealy, and W. L. Stutzman, "Spatial, polarization, and pattern diversity for wireless handheld terminals," *Antennas and Propagation, IEEE Transactions on*, vol. 49, no. 9, pp. 1271–1281, 2001.

[5] W. Lee and Y. Yeh, "Polarization diversity system for mobile radio," *Communications, IEEE Transactions on [legacy, pre - 1988]*, vol. 20, no. 5, pp. 912–923, 1972.

[6] S. Kozono, T. Tsuruhara, and M. Sakamoto, "Base station polarization diversity reception for mobile radio," *Vehicular Technology, IEEE Transactions on*, vol. 33, no. 4, pp. 301–306, 1984.

[7] R. G. Vaughan, "Polarization diversity in mobile communications," *Vehicular Technology, IEEE Transactions on*, vol. 39, no. 3, pp. 177–186, 1990.

[8] J. Jootar, J. F. Diouris, and J. R. Zeidler, "Performance of polarization diversity in correlated nakagami-m fading channels," *Vehicular Technology, IEEE Transactions on*, vol. 55, no. 1, pp. 128–136, 2006.

[9] L.-L. Yang and L. Hanzo, "Multicarrier ds-cdma: a multiple access scheme for ubiquitous broadband wireless communications," *Communications Magazine, IEEE*, vol. 41, no. 10, pp. 116–124, 2003.

[10] S. Kondo and B. Milstein, "Performance of multicarrier ds cdma systems," *Communications, IEEE Transactions on*, vol. 44, no. 2, pp. 238–246, 1996.

[11] L. Hanzo, L. L. Yang, E. L. Kuan, and K. Yen, *Multi-User Detection, Space-Time Spreading, Synchronisation, Networkingand Standards*. Chichester, England ; Hoboken, NJ: Wiley-IEEE Press, 2003.

[12] R. Prasad and S. Hara, "An overview of multi-carrier cdma," in *Spread Spectrum Techniques and Applications Proceedings, 1996., IEEE 4th International Symposium on*, vol. 1, 1996, pp. 107–114 vol.1.

[13] X. Gui and T. S. Ng, "Performance of asynchronous orthogonal multicarrier cdma system in frequency selective fading channel," *Communications, IEEE Transactions on*, vol. 47, no. 7, pp. 1084–1091, 1999.

[14] M. Nakagami, *The m-Distribution — A General Formula of Intensity Distribution of Rapid Fading*, ser. Statistical Methods in Radio Wave Propagation. Oxford, U.K.: Permagon, 1960.

[15] P. L'Ecuyer and C. Lemieux, "Quasi-monte carlo via linear shift-register sequences," vol. 1, 1999, pp. 632–639 vol.1.

[16] N. S. Correal and B. D. Woerner, "Enhanced ds-cdma uplink performance through base station polarization diversity and multistage interference cancellation," in *Global Telecommunications Conference, 1998. GLOBECOM 98. The Bridge to Global Integration. IEEE*, vol. 4, 1998, pp. 1905–1910 vol.4.

[17] R. M. Narayanan, K. Atanassov, V. Stoiljkovic, and G. R. Kadambi, "Polarization diversity measurements and analysis for antenna configurations at 1800 mhz," *Antennas and Propagation, IEEE Transactions on*, vol. 52, no. 7, pp. 1795–1810, 2004.

[18] R. U. Nabar, H. Bolcskei, V. Erceg, D. Gesbert, and A. J. Paulraj, "Performance of multiantenna signaling techniques in the presence of polarization diversity," *Signal Processing, IEEE Transactions on [see also Acoustics, Speech, and Signal Processing, IEEE Transactions on]*, vol. 50, no. 10, pp. 2553–2562, 2002.